

Figure S1. Treatment with auranofin (AF) and buthionine sulfoximine (BSO) reduces CD25 levels and activation of CD8⁺ T-lymphocytes *in vitro*. CD8⁺ T-cells were isolated from whole blood and left untreated or treated with AF (250 nM), BSO (250 μ M) or a combination of the two. At 24 hours post-treatment cells were activated with α -CD3 and α -CD28 antibodies. Panel A. Levels of CD25 and annexin V measured 48 hours post-activation. Panel B. Photographs taken at 72 hours post-activation.

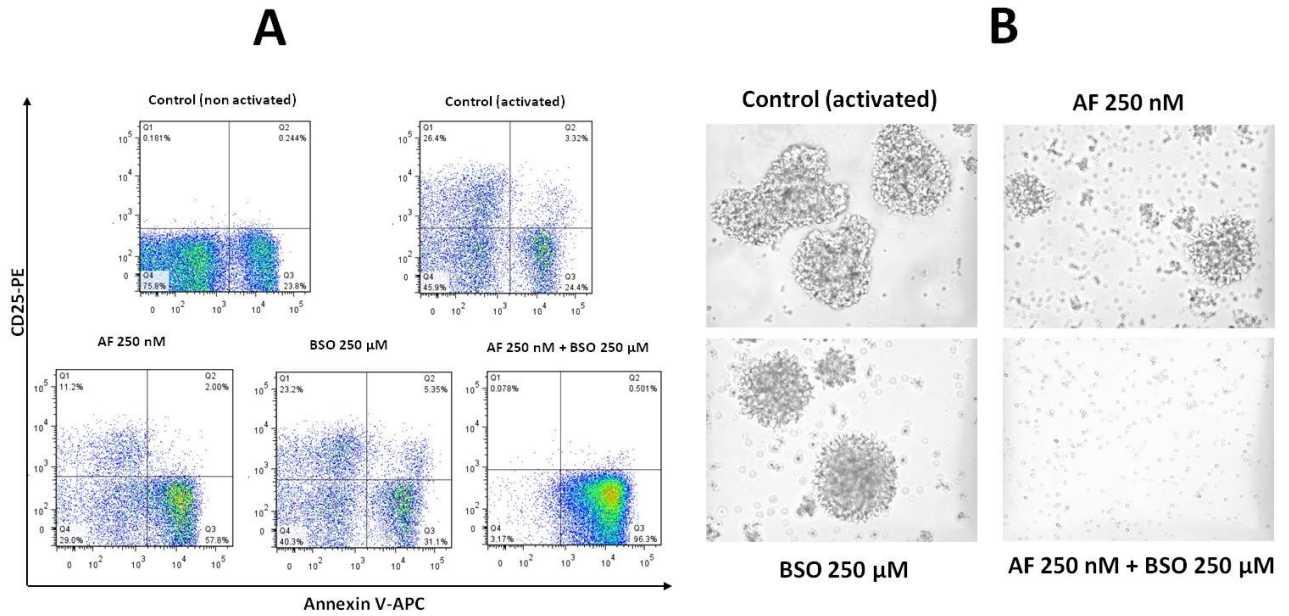


Figure S2: Treatment with auranofin and BSO reduces PHA-induced activation of T-lymphocytes *in vitro*. CD4⁺ and CD8⁺ T-cells were isolated from whole blood and left untreated or treated with auranofin (250 nM), BSO (250 μM), or a combination of the two. At 24 hours post-treatment, cells were activated with phytohemagglutinin (PHA). Upper panels: photographs of cell cultures taken at 72 hours post-activation. Lower panels: cell viability as measured with the MTS assay at 72 hours post-activation. Means ± SEM. * *P* < 0.05; ** *P* < 0.01.

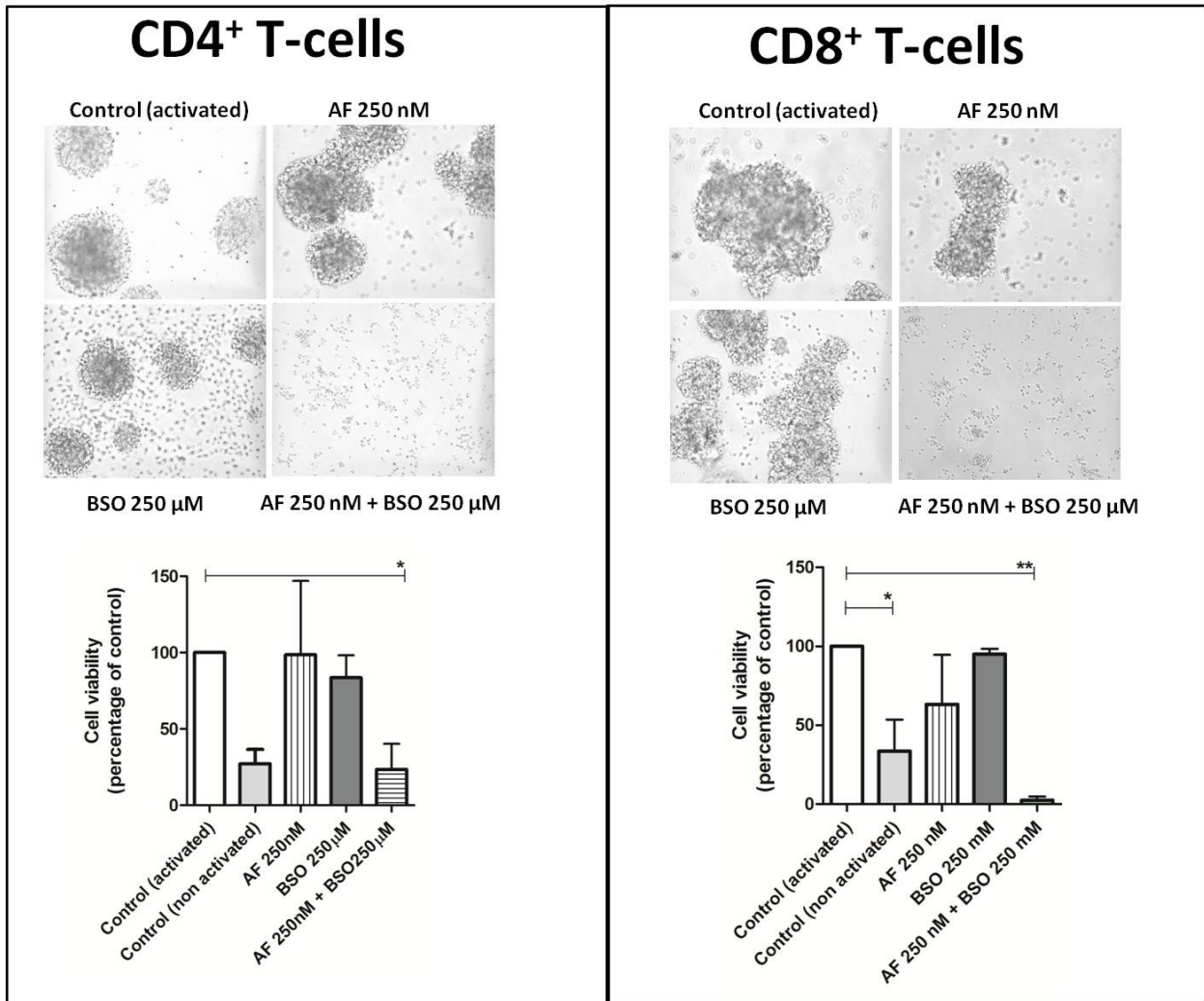


Figure S3. Comparison of the anti-Gag immune responses of macaques treated with ART/auranofin/BSO and control macaques. For all analyses, overlapping peptides spanning the entire Gag region were divided in two peptide pools comprising the N- and the C-terminal half of Gag, respectively. The analyses were performed by IFN- γ ELISpot on PBMCs. Data are expressed as spot forming cells (SFC) x million PBMC.

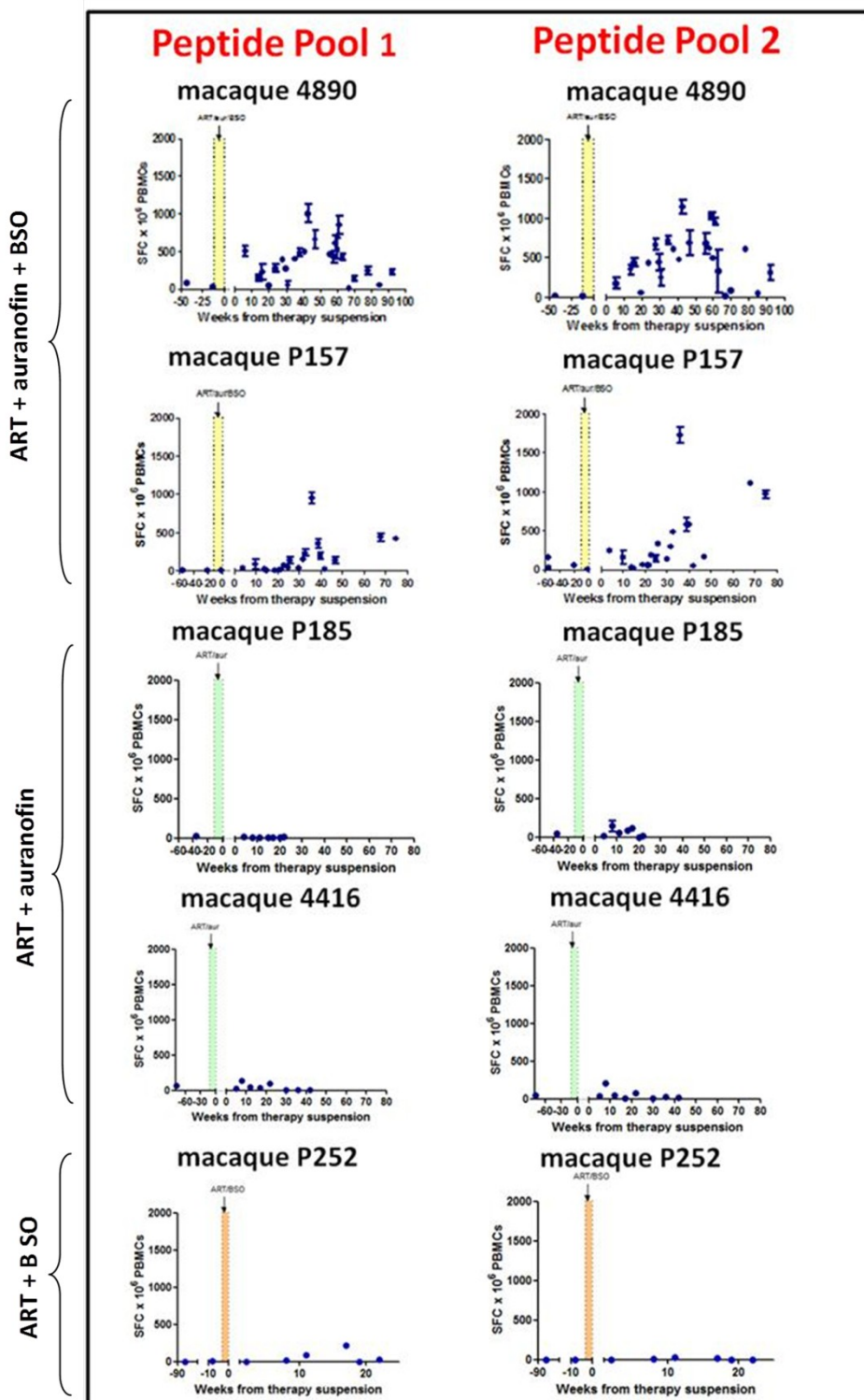


Figure S4: Dynamics of the immune responses elicited by HIV-1 Gag in the PBMCs of macaque 4890 following suspension of ART, auranofin and BSO. The analysis were performed by ELISpot on PBMCs stimulated with a pool of peptides spanning the entire HIV-1 Gag antigen. Data are expressed as spot forming cells (SFC) x million PBMC. ** $P < 0.01$

Crossreactivity to HIV-1 Gag

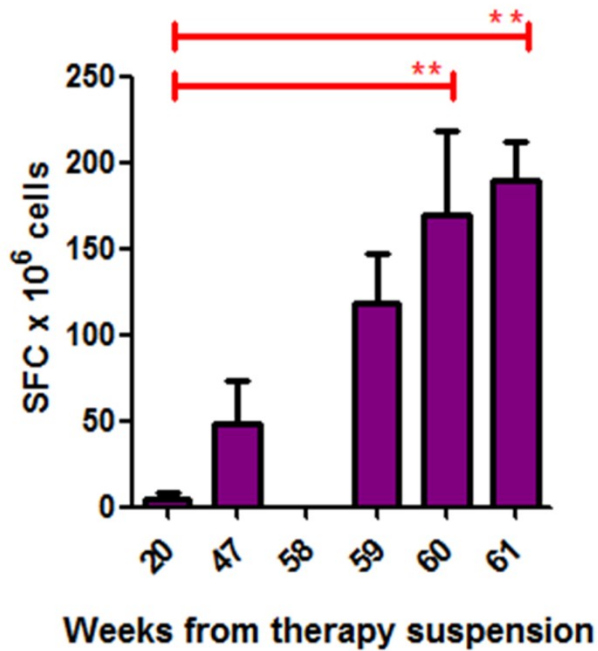


Figure S5. Immune responses against the conserved regions of the N-terminal half of SIVmac239 Gag. The analyses were performed by IFN- γ ELISpot. Macaque PBMCs were stimulated with a pool of peptides spanning the entire N-terminal half of Gag, and, separately, with smaller pools spanning two conserved regions identified in the N-terminal half (CR1 and CR2, see Text S1). Data are expressed as spot forming cells (SFC) x million PBMC. The ratio of conserved responses over total is calculated, for each time point, as a sum of the mean number of SFC detected when stimulating with CR1 and CR2 peptides divided by the mean number of SFC detected when stimulated with peptides spanning the N-terminal half of Gag.

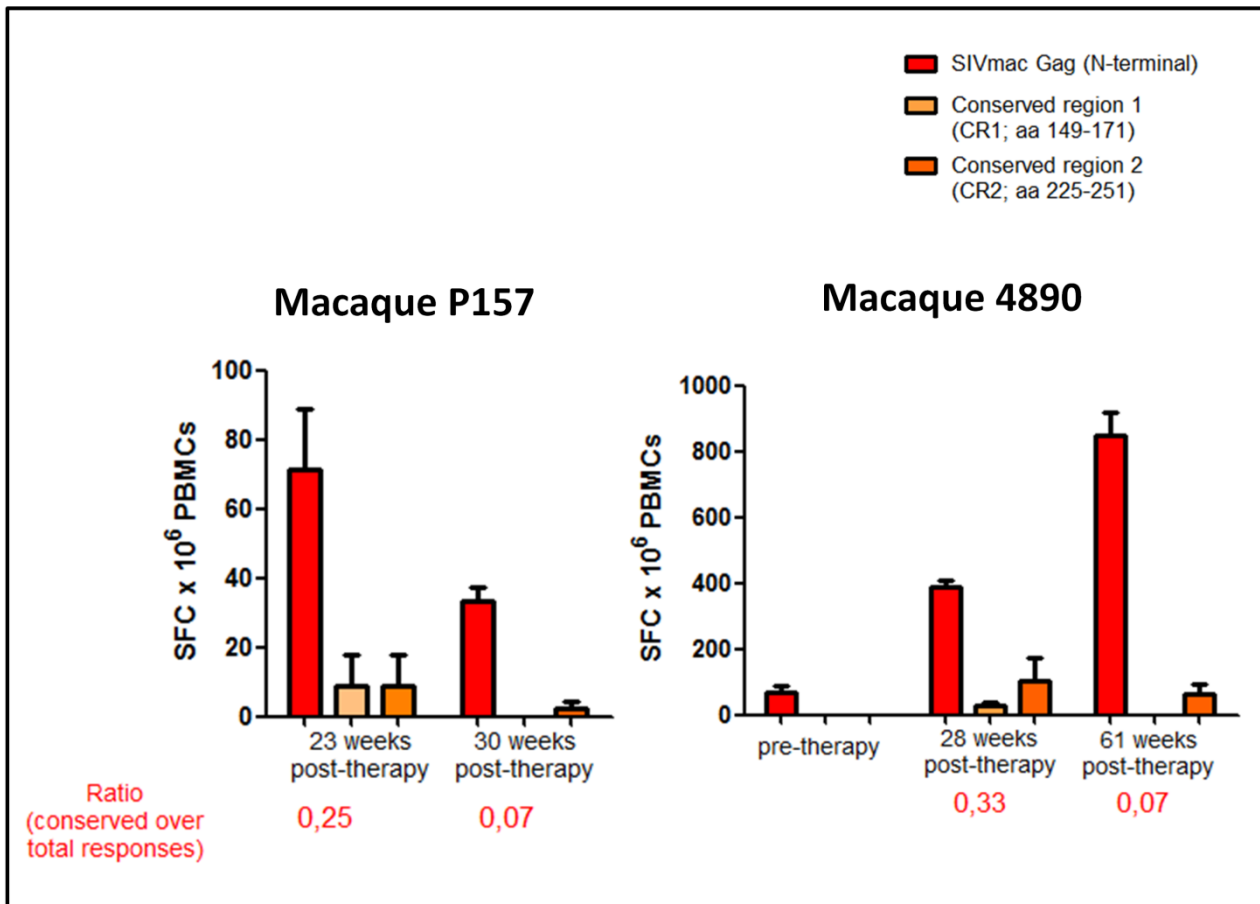


Figure S6: Neutralizing antibody titers of macaques treated with ART/auranofin/BSO and control macaques. Neutralizing antibody titers are expressed as the Log₂ plasma dilution required for 80% inhibition of a neutralization-sensitive (SIVmac251.6, green dots) and 50% inhibition of a neutralization-resistant (SIVmac251.30, blue dots) pseudotyped virus.

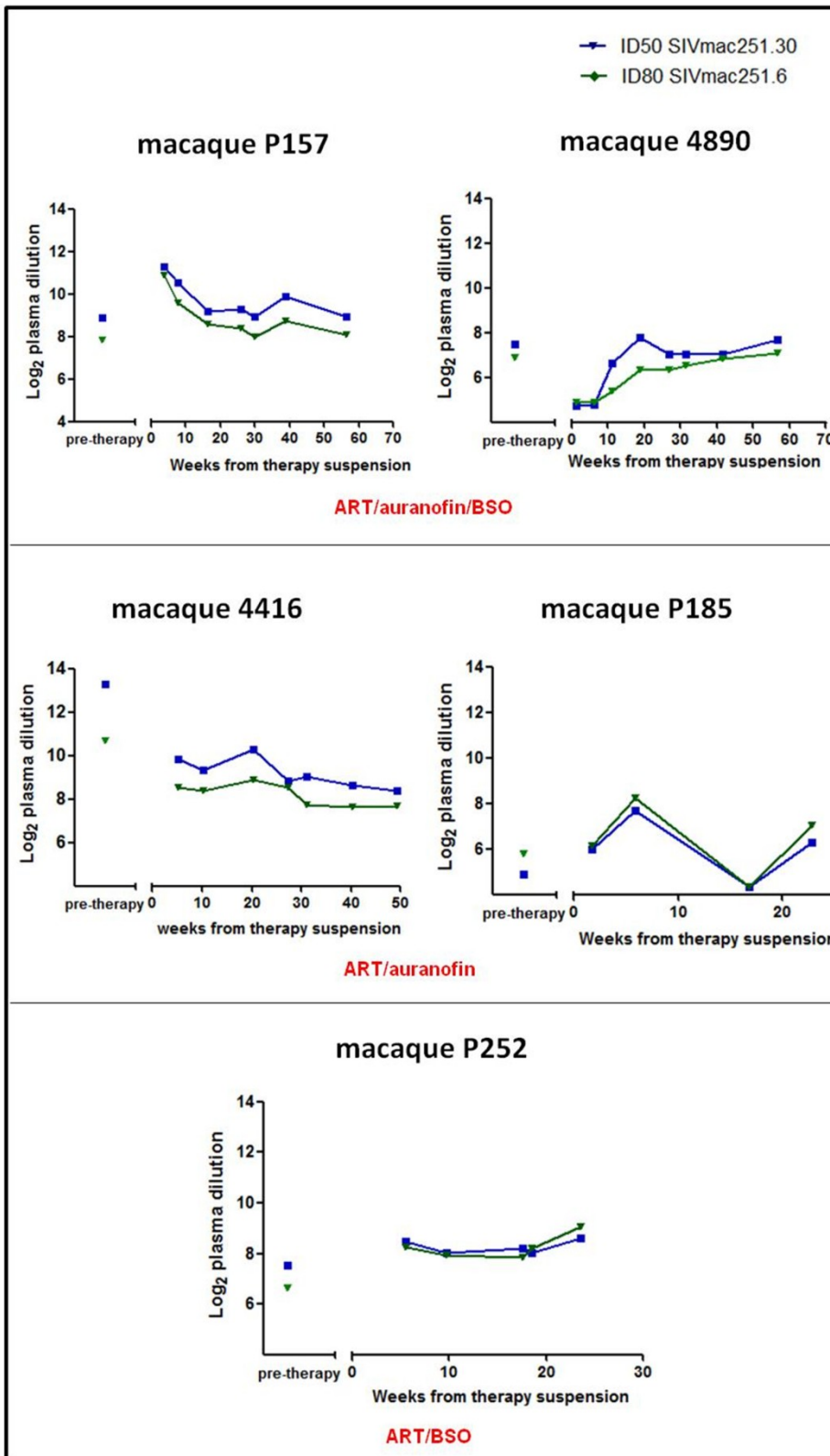


Figure S7: T-cell counts before and after CD8⁺ cell depletion in macaque P157. Means \pm SD are shown and were analyzed by unpaired *t*-test. *** $P < 0.0001$.

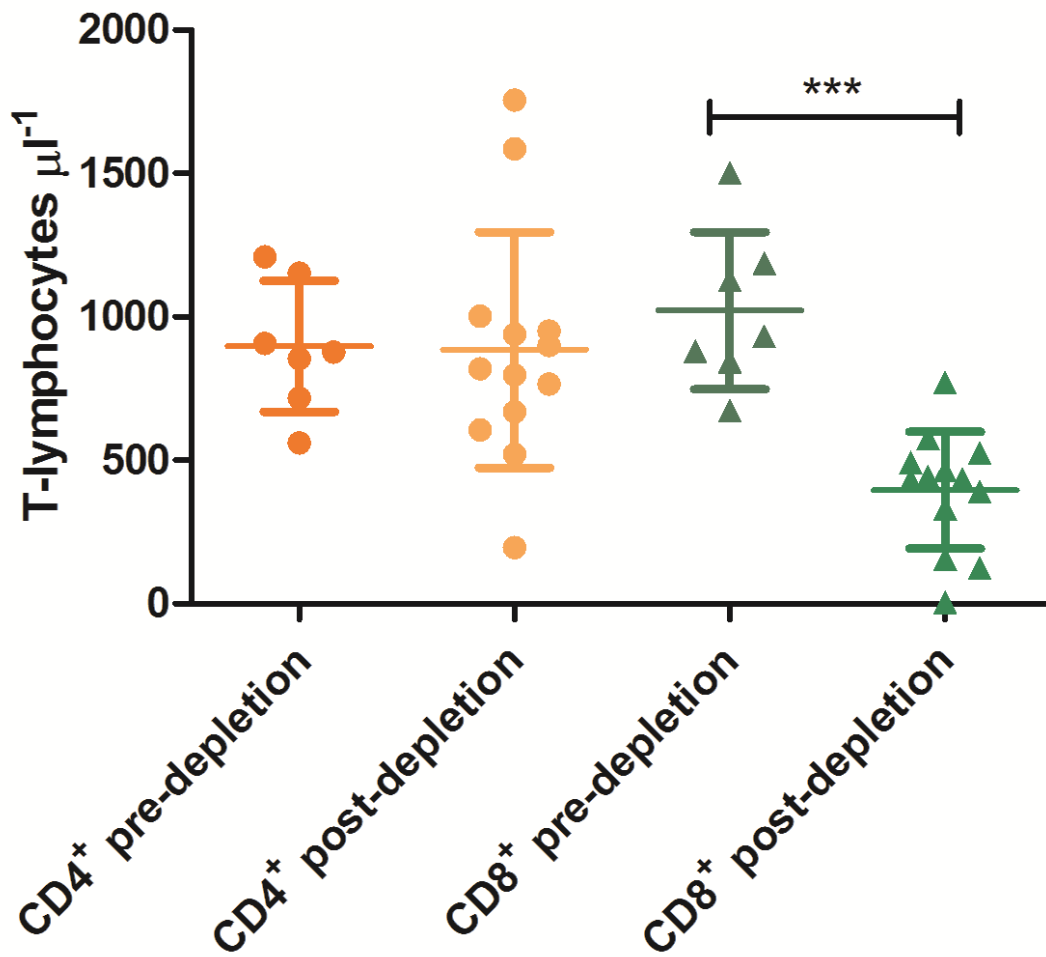


Figure S8: Long-term follow-up of viral DNA, CD4 counts and body weight of macaque 4890.
Data were analyzed by linear regression.

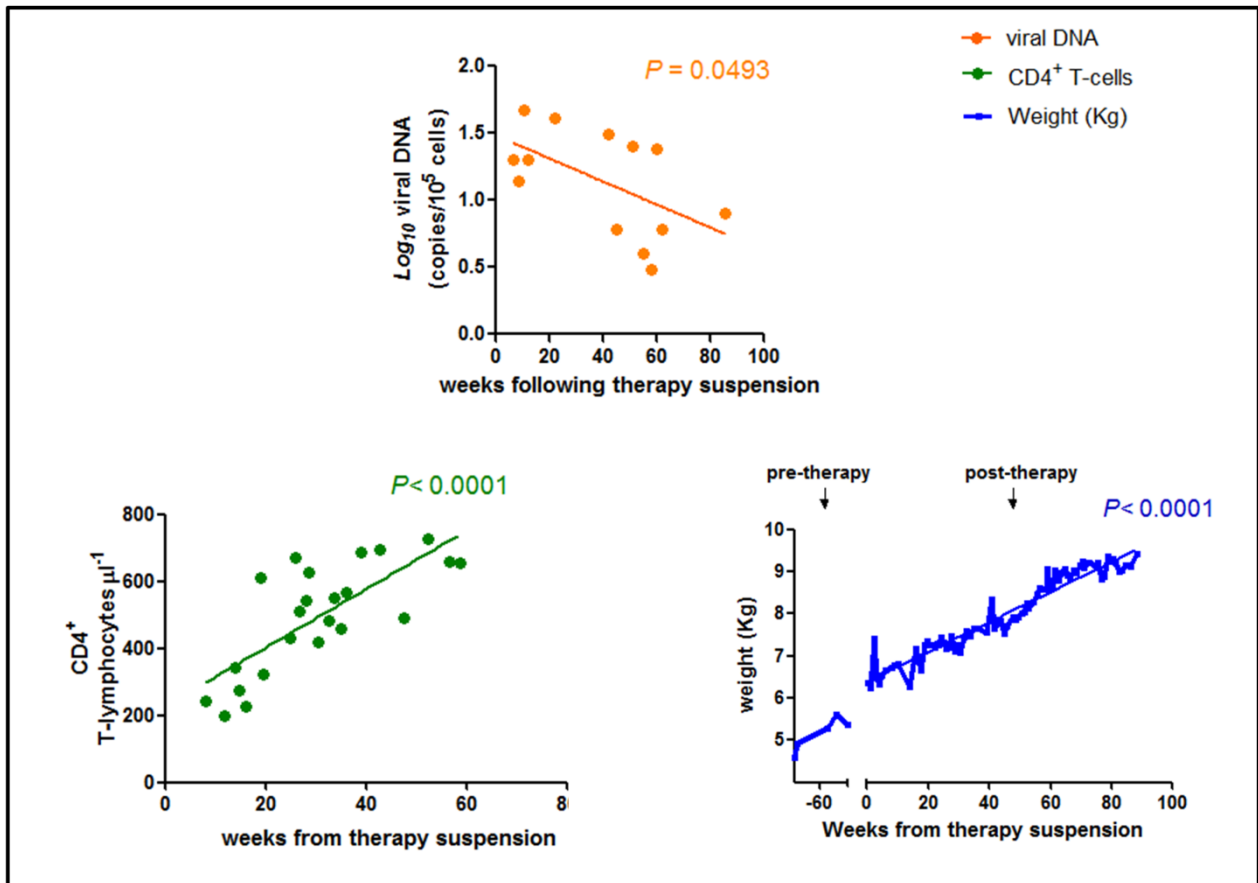


Table S1: Validations of viral nucleic acid quantification. Data were obtained in three different laboratories: Bioqual (using real-time PCR for both viral load and viral DNA; limits of detection $\approx 1.6 \text{ Log}_{10}$ copies of viral RNA/mL and 2 copies of viral DNA/ 5×10^5 cells), ABL (using NASBA for viral load and real-time PCR for viral DNA; limits of detection $\approx 1.7 \text{ Log}_{10}$ viral RNA copies/mL and 2 copies of viral DNA/ 10^6 cells), VGTI Oregon (using real-time PCR for viral load; limit of detection $\approx 2.3 \text{ Log}_{10}$ copies of viral RNA/mL). The coefficient of variation was calculated as the ratio between the standard deviation and the mean of the values available for a given time point.

	TIME POINT (weeks post-therapy)	BIOQUAL	ABL	VGTI Oregon	COEFFICIENT OF VARIATION
Macaque P157	40	-	4.37	3.64	12.89%
Macaque P157	58	3.86	4.32	4.05	5.67%
Macaque P157	61	4.04	-	3.98	1.06%
Macaque P157	67	-	3.42	4,20	14.48%
Macaque 4890	49	-	Undetectable (<1.70)	Undetectable (<2.30)	N.A.
Macaque 4890	51	-	4.14	Undetectable (<2.30)	N.A.
Macaque 4890	53	-	Undetectable (<1.70)	2.78	N.A.
Macaque 4890	55	-	Undetectable (<1.70)	2.87	N.A.
Macaque 4890	59	-	3.14	2.53	15.21%
Macaque 4890	60	-	Undetectable (<1.70)	2.71	N.A.
Macaque 4890	64	-	2.77	2.40	10.12%
Macaque 4890	78	-	Undetectable (<1.70)	2.49	N.A.
Macaque 4890	79	-	Undetectable (<1.70)	Undetectable (<2.30)	N.A.
Macaque 4890	83	-	Undetectable (<1.70)	Undetectable (<2.30)	N.A.
Macaque 4890	84	-	Undetectable (<1.70)	Undetectable (<2.30)	N.A.
Macaque 4890	88	-	Undetectable (<1.70)	Undetectable (<2.30)	N.A.
Macaque 4890	92	-	Undetectable (<1.70)	Undetectable (<2.30)	N.A.
Macaque 4890 (vDNA)	85	8	1) Undetectable and 2) 126 (Note: values in duplicate)	N.A.	N.A.

Table S2. Multivariate analysis of the correlation between therapeutic efficacy and selected parameters. A cohort of 19 chronically SIV-mac251-infected rhesus macaques was used for this retrospective analysis. Therapeutic efficacy was defined in terms of post-therapy viral load (VL) set point and Δ VL set point (*i.e.* the difference between the pre-therapy and the post-therapy viral load set points). The parameters selected to reveal potential correlations with therapeutic efficacy were selected to identify possible biases (*e.g.* CD4 nadir, pre-therapy VL set point) or contributors to the efficacy of the drugs administered (*e.g.* number of drugs simultaneously administered, total exposure to the drugs, number of therapeutic cycles). Non-canonical parameters (*i.e.* administration of a CD8⁺ cell-depleting antibody or of an unrelated drug such as mefloquine) were included as well to increase the potency of the analysis in detecting possible correlations.

Tests of Between-Subjects Effects

Source	Dependent Variable	Type I Sum of Squares	df	Mean Square	F	Sig.
Corrected Model	VLsetpoint-post	41.824 ^a	8	5.228	19.566	$P < 0.001$
	Δ VLsetpoint	20.890 ^b	8	2.611	9.494	$P = 0.001$
Intercept	VLsetpoint-post	262.761	1	262.761	983.397	$P < 0.001$
	Δ VLsetpoint	29.276	1	29.276	106.439	$P < 0.001$
N. of drugs simult. administered	VLsetpoint-post	3.748	1	3.748	14.028	$P = 0.004$
	Δ VLsetpoint	8.085	1	8.085	29.396	$P < 0.001$
N. of therapeutic cycles	VLsetpoint-post	10.077	1	10.077	37.713	$P < 0.001$
	Δ VLsetpoint	1.689	1	1.689	6.140	$P = 0.033$
VLsetpoint-pre	VLsetpoint-post	17.191	1	17.191	64.338	$P < 0.001$
	Δ VLsetpoint	.122	1	.122	.444	$P = 0.520$
CD4 nadir	VLsetpoint-post	3.833	1	3.833	14.346	$P = 0.004$
	Δ VLsetpoint	4.920	1	4.920	17.889	$P = 0.002$
α -CD8 mAb	VLsetpoint-post	6.362	1	6.362	23.809	$P = 0.001$
	Δ VLsetpoint	5.410	1	5.410	19.668	$P = 0.001$
mefloquine (unrelated drug)	VLsetpoint-post	.059	1	.059	.222	$P = 0.648$
	Δ VLsetpoint	.104	1	.104	.380	$P = 0.552$
Total exposure to drugs	VLsetpoint-post	.546	1	.546	2.044	$P = 0.183$
	Δ VLsetpoint	.551	1	.551	2.003	$P = 0.187$
Error	VLsetpoint-post	2.672	10	.267		
	Δ VLsetpoint	2.751	10	.275		
Total	VLsetpoint-post	307.258	19			
	Δ VLsetpoint	52.917	19			
Corrected Total	VLsetpoint-post	44.496	18			
	Δ VLsetpoint	23.641	18			

a. R Squared = .940 (Adjusted R Squared = .892)

b. R Squared = .884 (Adjusted R Squared = .791)

Text S1: Alignment of the amino acid sequences of the lentiviral Gag proteins employed for the ELISpot experiments. The alignment was performed using the CLUSTAL Ω (v. 1.2.0, EMBL-EBI) software. The Gag sequences used were derived from the following lentiviruses: 1) HIV-1; 2) SIVver; 3) SIVsab; 4) SIVmac239; 5) SIVsm (for a description of these viruses see main text). Highlighted are the four conserved regions of the SIVmac239 Gag that were separately tested in ELISpot experiments.

```

HIV-1          MGARASVLSGGKLDWRWEKIRLRPGGKKKYKPKHIVWASRELERFAVNPGLLETSEGCRCQI
SIVver        MGAAATNALNRRQLDKFEHIRLRPTGKKKYQIKHLLIWAGKEMERFGLHERLLESEHGCKKI
SIVsab        MGASNSVLSGRKLDAFEVLVLRPNPNGKKKYKLRHLVWASKELDRFGLSANLLETKEGVVKI
SIVmac239     MGARNVLSGKKADELEKIRLRPNPNGKKKYMLKHHVVAANELDRFGLAESLLENKEGCQKV
SIVsm        MGARGSVLSGKKADELEKIVLRPGRGKKYMLKHIWAARELDRFGSAESLLESKEGCQRI
***  *.*  : * * :**** *:*** ::*:*..*:*:*  *..*..*  ::
HIV-1          LGQLQPSLQGTGSEECRSLYNTVATLYCVHQRIEIKDTKEALDKIKKEEQNKSKKKAQ----
SIVver        IEVLYPLEPTGSEGLKSLFNLCVLCVHDKDVKDTEBAVAIVRQCCHLVEKERNNAERN
SIVsab        LSVLLPLVPTGSENLIALFNLCVLCVHAEIKVKDTEEAQTKIKQEVPLEMTESA----
SIVmac239     LSVLAPLMPTGSENLKSLYNTVAVIWCIAHEEKVKHTEEAQKIVQRHLVETGTTE----
SIVsm        LAVLAPLMPTGSENLKSLFSTVCVWVWCLHAEMKVKDTEEAQKTVQSHLVVESGTAE----
:  * *  ****  *:..  ..:  *: *  :*:.*:*  *:
HIV-1          -----QAAADTGHSSQVSQNYPIVQNIQGMVHQAISPRTLNAWVKVVEE
SIVver        TTESSGQ-----KKNDKGVTVPPGGSQNFPAQ-QQGNAWIHVPLSPRTLNAWKAVEE
SIVsab        -TVTSSGQKQELQGGKNEAIAPSGGGSNYPV-SVNNQWVHQPLSPRTLNAWVKVIEE
SIVmac239     -T-----M--PKTSRPTAPSSGRGGNYPVQ-QIGGNYVHLPLSPRTLNAWVKVVEE
SIVsm        -K-----L--PAQSRPTAPPS--GGNYPVQ-QVGNNYVHTPLSPRTLNAWVKVVEE
      .  *: *  .  *  :  *  :*****  *:
HIV-1          KAFSPEVPMFSALESGATPQDLNMTLNTVGGHQAMQMLKETINEEAAEWDRVHPVHAG
SIVver        KKFGEIVPMFQALSEGCTPYDINQMLNVLGDHGALQIVKEIINEEAAQWDIAHPPAG
SIVsab        KKFSAEVVPMFSALEGAIPYDINQMLNAVGDHGALQIVKDVINEEAADWDLRHPPPQQ
SIVmac239     KKFGEVVPFQALSEGCCPYDINQMLNLCVGDHQAMQIIRDVINEEAADWDLQHPQ---
SIVsm        KKFGEVVPFQALSEGCTPYDINQMLNLCVGEHQAMQIIREIINEEAADWDLQHPGQQ
*  *  .  *: *  *  *  *  *  *  *  *  *  *  *  *  *  *  *  *  *  *  *  *
HIV-1          P-IAPGQMRPRGSDIAGTTSTLQEQIGWMTN-NPPIPVGGEIYKRWIILGLNKIVRMYSP
SIVver        P-LPAGQLRDRPRGSDIAGTTSTVQEQLEWIYTANPRVDVGAIRRWIILGLQKCVKMYNP
SIVsab        P-PAQGVLRREPQGSADIAGTTSTIPEQIEWTTRAQNAINVGNIYKRWIILGLQKCVKMYNP
SIVmac239     PAPQGGQLPEPSGSDIAGTTSTVDEQIQWYRQONPLPVGNIIYRPWIQLGLQKCVRMYNP
SIVsm        PAQAGGLREPSGSDIAGTTSTPSEQIEWMYRAQNPVPVGDIIYRWIQLGLQKCVRMYNP
*  *  .  *: *  *  *  *  *  *  *  *  *  *  *  *  *  *  *  *  *  *  *  *
HIV-1          TSILDIRQGPKEPFRDYDRFYKTLRAEQASQEVKNWMTETLLVQNANPDCKTILKALGP
SIVver        VSVLDIRQGPKEAFKDYDRFYKAIKRAEQASGEVKNWMTESLLIQNANPDCKVILKGLGM
SIVsab        VNLDIKQGPKEPFDYDRFYKALRAEQTDPAVKNWMTQSLLIQNANPDCKTVLRGLGM
SIVmac239     TNILDVKQGPKEPFQSYVDRFYKSLRAEQTDPAVKNWMTQTLTIQNANPDCKLVKGLGV
SIVsm        TNILDVKQGPKEPFQSYVDRFYKSLRAEQTDPAVKNWMTQTLTIQNANPDCKLVKGLGM
.  .  *:..*:*:*  *  *  *  *  *  *  *  *  *  *  *  *  *  *  *  *  *  *  *  *
HIV-1          AATLEEMLTACQGVGGPGHKARVLAEMASQVNTSATIM-----MQRGNFRNQR
SIVver        HPTLEEMLTACQGVGGPSYKAKVMAEMMQNSQNMNQ---QG-----GQRGRPR
SIVsab        NPTLEEMLTACQGVGGQHKARLMAEAMSAAFQQQTMGNIFVQQGARPKGLPRGGQRPIN
SIVmac239     NPTLEEMLTACQGVGGPGQKARLMAEALKEALAPVPIP--F-AA-----AQRGRPR
SIVsm        NPTLEEMLTACQGVGGPGQKARLMAEAMKDALTGSLVAAQFRGA-----AFGQGNK
      *****  *****  *  *  :  *  *  :
HIV-1          KIVKCFNCGKEGH IARNCRAPRKGCKWKCGKEGHQMKDCTERQANFLGKIWPSYKGRPGN
SIVver        PPVKCYNCGKFGHMQRQCPEPRKMRCLKCGKPGHLAKDCRG-QVNFLGYG-RWMAKPRN
SIVsab        PNLKCYNCGKGTGHIARFCRAPRRQGCWKCGSPDHQMKDCQK-QVNFLGFY-PWGRGKPRN
SIVmac239     KPIKCNCGKEGH IARNCRAPRKGCKWKCGKEGHQMKDCTERQANFLGKIWPSYKGRPGN
SIVsm        PIIRCFNCGKGTGHSARQCRAPRRKGCKWKCGEEGRIQANCPNQKAGFLGLG-PWGK-KPRN
      ::*:*:*  *  *  *  *  *  *  *  *  *  *  *  *  *  *  *  *  *  *  *  *
HIV-1          FLQS--RPEPTAPPEESFRS-----GNET
SIVver        FPAATLQVEPTAPP-----PPSPYDPAKKLLQYADKQGQLEQR
SIVsab        FPLTSVR--PTAPPMERDYSRPEENWYANRPPTAGSGPDDPATALLKQYAVQGRQRQSR
SIVmac239     FPMQVH--QGLMP-----TAPPEDPAVDLLKNYMLQKQOREKQ
SIVsm        FPMQTTS--LTP-----SA-PPDPAARIVKEYLEKAQ----RE
*
HIV-1          TTPPKQKEPIDKELYPLTSLRSLFNDPSSQ
SIVver        KKPPAVNPDWT---EGYSLNSLFGEDQ---
SIVsab        QSSPPQQS PYE---EAYSSLRSLFSGEDQ---
SIVmac239     RE--SREKPYKEVTEDLLHNSLFGGDQ---
SIVsm        KT--RRSRPYKEVTEDLLHNSLFGEDQ---
      .
      *  *  *  *  *  *

```

Grey: conserved region 1 (CR1)

Blue: conserved region 2 (CR2)

Yellow: conserved region 3 (CR3)

Green: conserved region 4 (CR4)

Text S2. Viral load control in the macaques that had received auranofin and BSO does not depend on the genetic background of the host.

We analyzed the contribution of the baseline MHC background of the macaques to the functional cure-like condition that we observed. As the class I MHC haplotypes are the only widely recognized major determinants of the immune responses against the virus [1], we focused our analysis on these haplotypes and their main target sequences in SIVmac251. As shown in Table 1 of the main text, macaques P157 and 4890 did not share any common MHC class I haplotype (they were positive for Mamu-A*11 and Mamu-A*02/B*17, respectively). We conducted ELISpot analyses in order to check the cell-mediated immunity of these macaques against the restricted epitopes of their MHC I haplotypes that are associated with immunodominant responses. We found that macaque P157 did not display any cell-mediated response to Env and Pol (*i.e.* the viral components encompassing the main targets of Mamu-A*11 [2,3]). Macaque 4890 did show anti-Env responses (data not shown), but did not show any significant responses to the Mamu-B*17 specific epitope within Env (sequence analyzed: YGWSYFHEAVQAVWRSATE, see Ref [4]). The same macaque showed no significant responses to the other Mamu-B*17 restricted epitopes within Nef (sequences analyzed: SGPGIRYPKTFGWLWKLVP and DEEHYLMHPAQTSQWDDPW, see Ref [4]) and Vif (sequence analyzed LQEGSHLEVQGYWHLTPEK, see Ref [4]). Although the main immune response of macaque 4890 was directed towards a C-terminal portion of SIV p27 (Fig. 5), there were in general high anti-Gag responses also towards the N-terminal portion (Fig. S3), thus rendering it difficult to determine, through ELISpot, the contribution of immune responses against the preferential target of the other MHC I haplotype of 4890, *i.e.* Mamu-A*02. Despite the low viral loads displayed by this animal, it was possible to sequence the N-terminal portion of Gag. The results showed that the virus bore a mutation in the immunodominant Mamu-A*02 epitope in Gag, *i.e.* GY9 [5-7] (see below). This mutation (E73D) shortens an important anchor of the peptide to the MHC I Mamu-A*02 molecule (see 3D structure: PDB accession: [3JTS](#)). Taken together, these results strongly support the view that the genetic background of the animals may not have

influenced the profound change in disease progression observed after the animals had been treated with the auranofin/BSO combination.

Mutations detected in the N-terminal portion of Gag from plasma virus of macaque 4890 following therapy suspension.

SIVmac251 Gag consensus

MGARNSVLSGKKADELEKIRLRPGGKKKYMLKHVVWAANELDRFGLAESLLENKEGCQK
ILSVLAPLVPTGSENLSLYNTVCVIWCIAHEEKVKHTEEAKQIVQRHLVVETGTAETMPK
TSRPTAPSSGRGGNYPVQQIGGNYVHLPLSPRTLNAWVKLIEEKKFGAEVVPGFQALSEGC
TPYDINQMLNLCVGDHQAAMQIIR

Macaque 4890: 5 weeks post-therapy

MGARNSVLSGKKADELEKIRLRPGGKKKYMLKHVVWAANELDRFGLAESLLENKEGCQK
ILSVLAPLVPTGSDNLKSLYNTVCVIWCIAHEEKVKHTEEAKQIVQRHLVVETGTAETMPK
TNRPTAPSSGRGGNYPVQQIGGNYVHLPLSPRTLNAWVKLIEEKKFGAEVVPGFQALSEGC
TPYDINQMLNLCVGDHQAAMQIIR

Macaque 4890: 20 weeks post-therapy

MGARNSVLSGKKADELEKIRLRPGGKKKYMLKHVVWAANELDRFGLAESLLENKEGCQK
ILSVLAPLVPTGSDNLKSLYNTVCVIWCIAHEEKVKHTEEAKQIVQRHLVVETGTAETMPK
TSRPTAPSSGRGGNYPVQQIGGNYVHLPLSPRTLNAWVKLIEEKKFGAEVVPGFQALSEGC
TPYDINQMLNLCVGDHQAAMQIIR

Macaque 4890: 68 weeks post-therapy

MGARNSVLSGKKADELEKIRLRPGGKKKYMLKHVVWAANELDRFGLAESLLENKEGCQK
ILSVLAPLVPTGSDNLKSLYNTVCVIWCIAHEEKVKHTEEAKQIVQRHLVVETGTAETMPK
TNRPTAPSSGRGGNYPVQQIGGNYVHLPLSPRTLNAWVKLIEEKKFGAEVVPGFQALSEGC
TPYDINQMLNLCVGDHQAAMQIIR

E73D

S122N

S122N (likely present)

References

1. **Goulder PJ, Watkins DI.** 2008. Impact of MHC class I diversity on immune control of immunodeficiency virus replication. *Nat Rev Immunol.* **8**(8):619-30. Review.
2. **Evans DT, Jing P, Allen TM, O'Connor DH, Horton H, Venham JE, Piekarczyk M, Dzuris J, Dykhuzen M, Mitchen J, Rudersdorf RA, Pauza CD, Sette A, Bontrop RE, DeMars R, Watkins DI.** 2000. Definition of five new simian immunodeficiency virus cytotoxic T-lymphocyte epitopes and

their restricting major histocompatibility complex class I molecules: evidence for an influence on disease progression. *J Virol.* **74**(16):7400-10.

3. **Sette A, Sidney J, Bui HH, del Guercio MF, Alexander J, Loffredo J, Watkins DI, Mothé BR.** 2005. Characterization of the peptide-binding specificity of Mamu-A*11 results in the identification of SIV-derived epitopes and interspecies cross-reactivity. *Immunogenetics.* **57**(1-2):53-68.
4. **Weinfurter JT, May GE, Soma T, Hessel AJ, León EJ, Macnair CE, Piaskowski SM, Weisgrau K, Furlott J, Maness NJ, Reed J, Wilson NA, Rakasz EG, Burton DR, Friedrich TC.** 2011. Macaque long-term nonprogressors resist superinfection with multiple CD8⁺ T cell escape variants of simian immunodeficiency virus. *J Virol.* **85**(1):530-41.
5. **Vogel TU, Friedrich TC, O'Connor DH, Rehrauer W, Dodds EJ, Hickman H, Hildebrand W, Sidney J, Sette A, Hughes A, Horton H, Vielhuber K, Rudersdorf R, De Souza IP, Reynolds MR, Allen TM, Wilson N, Watkins DI.** 2002. Escape in one of two cytotoxic T-lymphocyte epitopes bound by a high-frequency major histocompatibility complex class I molecule, Mamu-A*02: a paradigm for virus evolution and persistence? *J Virol.* **76**(22):11623-36.
6. **Loffredo JT, Sidney J, Wojewoda C, Dodds E, Reynolds MR, Napoé G, Mothé BR, O'Connor DH, Wilson NA, Watkins DI, Sette A.** 2004. Identification of seventeen new simian immunodeficiency virus-derived CD8⁺ T cell epitopes restricted by the high frequency molecule, Mamu-A*02, and potential escape from CTL recognition. *J Immunol.* **173**(8):5064-76.
7. **Feng Y, Qi J, Zhang H, Wang J, Liu J, Jiang F, Gao F.** 2005. X-ray crystallographic characterization of rhesus macaque MHC Mamu-A*02 complexed with an immunodominant SIV-Gag nonapeptide. *Acta Crystallogr Sect F Struct Biol Cryst Commun.* **62**(Pt 1):13-5.